Chromium ethylene polymerization catalysts bearing sterically enhanced α,α′-bis(imino)-2,3:5,6-bis(pentamethylene)pyridines: tuning activity and molecular weight

Chantsalnyam Bariashir,[a,b] Zheng Wang,[a,b] Gregory A. Solan,*[a,c] Chuanbing Huang,[a,b] Xiang Hao,[a] and Wen-Hua Sun*[a,b,d]

[a] Key Laboratory of Engineering Plastics and Beijing National Laboratory for Molecular Science, Institute of Chemistry, Chinese Academy of Sciences, Beijing 100190, China.

[b] CAS Research/Education Center for Excellence in Molecular Sciences, University of Chinese Academy of Sciences, Beijing 100049, China.

[c] Department of Chemistry, University of Leicester, University Road, Leicester LE1 7RH, UK.

[d] State Key Laboratory for Oxo Synthesis and Selective Oxidation, Lanzhou Institute of Chemical Physics, Chinese Academy of Sciences, Lanzhou 730000, China.

* Correspondence: whsun@iccas.ac.cn and gas8@leicester.ac.uk

Abstract

The *ortho*-benzhydryl-substituted α,α'-bis(arylimino)-2,3:5,6-bis(pentamethylene)pyridine-chromium(III) chlorides, [2,3:5,6-{$C_4H_8C(N(2\text{-}R^1\text{-}4\text{-}R^2\text{-}6\text{-}(CHPh_2)C_6H_2)\}_2C_5HN$]$CrCl_3$ [R^1 = R^2 = Me **Cr1**, R^1 = Me, R^2 = $CHPh_2$ **Cr2**, R^1 = Et, R^2 = $CHPh_2$ **Cr3**, R^1 = *i*-Pr, R^2 = $CHPh_2$ **Cr4**, R^1 = Cl, R^2 = $CHPh_2$ **Cr5**, R^1 = F, R^2 = $CHPh_2$ **Cr6**], differing in the electronic and/or steric properties of their aryl-R^1 and -R^2 groups, have been prepared by a one-pot template approach involving α,α'-dioxo-2,3:5,6-bis(pentamethylene)pyridine, the corresponding aniline and $CrCl_3(THF)_3$ in acetic acid. The molecular structure of six-coordinate **Cr1** reveals the carbocyclic-fused *N,N,N*-ligand to adopt a *mer* configuration with the puckered sections of the two fused rings arranged mutually *cis*. On activation with MAO or MMAO, **Cr1 - Cr6** displayed high activities (up to 1.83×10^6 g (PE) mol^{-1} (Cr) h^{-1}) for the polymerization of ethylene with the MAO-promoted polymerizations in most cases more productive than with MMAO. In general, the chromium complexes appended with *ortho*-halide substituents (**Cr6** (F)) and (**Cr5** (Cl)), proved the most active with the overall order being: **Cr6** > **Cr5** > **Cr1** > **Cr2** > **Cr3** > **Cr4**. All catalysts formed linear polyethylene displaying a wide range of molecular weights (from 2.17 – 300.4 kg mol^{-1}) that were highly dependent on the nature of the *ortho*-R^1 substituent with fluoride **Cr6** forming the lowest molecular weight and the most sterically demanding **Cr4** (*i*-Pr) the highest.

Keywords: ethylene polymerization; chromium precatalysts; α,α'-bis(arylimino)-2,3:5,6-bis(pentamethylene)pyridine; electronic and steric effects

Introduction

The application of chromium catalysis in ethylene oligomerization and polymerization [1-12] represents a well documented research area with key examples including the heterogeneous Phillips catalyst [13-18] used for the manufacture of high density polyethylene (HDPE) and an assortment of different homogeneous systems for generating 1-hexene [3-5,19-24] and/or 1-octene [6,9,25-28]. Indeed, the mechanism of catalysis by which such chromium complexes operate has been subject of multiple investigations [2]. Elsewhere, molecular chromium complexes ligated with a raft of different neutral *N,N,N* ligands, such as triazacyclohexane [29-30], bis(imino)pyridine [31-34], (2-pyridylmethyl)amine [35], bis(oxazolinyl)pyridine [36], bis(benzimidazolyl)pyridine [37-38], tris(pyrazolyl)methane [39] and 2,6-bis(azolylmethyl)pyridine [40], have all been reported. In particular, the bis(imino)pyridine family of chromium precatalysts (**A**, Chart 1) have emerged as being particularly productive in ethylene oligomerization and/or polymerization [31-34,40, 41-46].

Over the last five years or so, we have been interested in the development of bis(imino)pyridines fused with carbocylic groups and have noted how such structural modifications can influence the performance of their iron and cobalt polymerization catalysts [47]. More recently, we have extended these studies to include chromium and have noted how singly fused ligands such as those seen in **B** – **D** (Chart 1) affect not only the catalytic activity and thermal stability but also the molecular weight of the polymer [48-50]. In addition, chromium catalysts bearing doubly fused α,α'-bis(arylimino)-2,3:5,6-bis(pentamethylene)pyridines (**E**, Chart 1) are synthetically accessible and have been shown to serve as highly active catalysts for generating strictly linear low molecular weight polyethylene waxes (M_w: 1.6 - 3.0 kg mol^{-1}) [51].

<Chart 1>

Given the tendency of **E** (Ar = 2,6-Me_2Ph, 2,6-Et_2Ph, 2,6-$^{i}Pr_2$Ph, 2,4,6-Me_3Ph, 2,6-Et_2-4-MePh, Chart 1) to promote the formation of low molecular polymers [51], we explore in this article how *ortho*-benzhydryl substitution to the same fused *N,N,N*-ligand framework can impact on both molecular weight and overall catalytic performance. Elsewhere, the introduction of such sterically demanding aryl substituents has been demonstrated to have beneficial effects on the thermal stability and catalytic performance of late transition metal polymerization catalysts (*e.g.*, Fe, Co, Ni) as well on the molecular weight of the resulting polyethylenes [47,52]. In particular, we target chromium precatalysts of type **F** (Chart 1) that contain *N*-aryl groups *ortho*-substituted with both a $CHPh_2$ and a sterically and electronically variable R^1 group (Me, Et, i-Pr, Cl, F); variations in the *para*-R^2 group presents an alternative point of interest (Me *vs.* $CHPh_2$). An in-depth catalytic

evaluation is then conducted to ascertain the effects of co-catalyst, temperature, time and pressure on the catalytic activity as well as the polymer properties (*e.g.* molecular weight and dispersity); these findings are then compared with data previously reported for benzhydryl-free **E** (Chart 1). In addition, the full synthetic and characterization details for all chromium(III) complexes are disclosed.

Experimental section

General considerations

All manipulations involving air and moisture sensitive compounds were carried out under a nitrogen atmosphere using standard Schlenk techniques. Toluene was refluxed over sodium and distilled under nitrogen prior to use. Methylaluminoxane (MAO, 1.46 M solution in toluene) and modified methylaluminoxane (MMAO, 1.93 M in n-heptane) were purchased from Akzo Nobel Corp. High purity ethylene was purchased from Beijing Yansan Petrochemical Co. and used as received. Other reagents were purchased from Aldrich, Acros or local suppliers. FT-IR spectra were recorded on a Perkin-Elmer System 2000 FT-IR spectrometer. Elemental analysis was carried out using a Flash EA 1112 micro-analyzer. Molecular weights and molecular weight distributions (M_w/M_n) of the polyethylenes were determined by Gel Permeation Chromatography (GPC) using a PL-GPC220 instrument at 150 ºC with 1,2,4-trichlorobenzene as the solvent. The thermograms for the crystallization and melt processes for the polymers were recorded using a differential scanning calorimeter (DSC, TA-Q2000) under a nitrogen atmosphere. Typically, a sample of about 5.0 mg was heated to 140 ºC at a rate of 20 ºC/min and kept for 2 min at 140 ºC to remove the thermal history and then cooled at a rate of 20 ºC/min to -40 ºC. The ^{13}C NMR spectra of the polyethylenes were recorded on a Bruker DMX 300 MHz instrument at 135 ºC in deuterated 1,1,2,2-tetrachloroethane-d_2 with TMS as an internal standard; δ values are given in ppm and *J* values in Hz. The compounds, α,α'-dioxo-2,3:5,6-bis(pentamethylene)pyridine [53-54], 2,4-dimethyl-6-benzhydrylaniline, 2-methyl-4,6-dibenzhydrylaniline, 2-ethyl-4,6-dibenzhydrylaniline, 2-isopropyl-4,6-dibenzhydrylaniline, 2-chloro-4,6-dibenzhydrylaniline and 2-fluoro-4,6-dibenzhydrylaniline were prepared using literature procedures [55,56]. $CrCl_3(THF)_3$ was prepared using the literature route [57,58].

Preparation of [2,3:5,6-{$C_4H_8C(N(2\text{-}R^1\text{-}4\text{-}R^2\text{-}6\text{-}(CHPh_2)C_6H_2)\}_2C_5HN$]$CrCl_3$

(a) $R^1 = R^2$ = Me **Cr1**. A suspension of α,α'-dioxo-2,3:5,6-bis (pentamethylene)pyridine (0.243 g, 1.0 mmol), 2,4-dimethyl-6-dibenzhydrylamine (1.150 g, 4.0 mmol) and $CrCl_3(THF)_3$ (0.374 g, 1.0

mmol) in glacial acetic acid (10 mL) was stirred and heated to reflux for 6 h. Once cooled to room temperature, diethyl ether (30 mL) was added to precipitate a solid which was filtered and collected. This solid was then re-dissolved in methanol (50 mL) and the solution concentrated to a minimum volume (*ca.* 5 mL). Diethyl ether was re-added to induce precipitation and the resulting solid collected by filtration and dried under reduced pressure to give **Cr1** as a green powder (0.65 g, 76%). FT-IR (KBr, cm^{-1}): $\tilde{\nu}$ = 2928 (w), 2864 (w), 1609 (s, $\nu_{C=N}$), 1522 (w), 1494 (s), 1449 (s), 1352 (m), 1244 (s), 1204 (m), 1156 (m), 1083 (m), 1032 (m), 967 (w), 917 (m), 863 (w), 782 (w), 742 (w), 699 (s). Anal. calc. for $C_{57}H_{55}Cl_3CrN_3$ (940.93): C, 72.80; H, 5.90; N, 4.47. Found C, 72.69; H, 5.90; N, 4.45%.

(b) R^1 = Me, R^2 = $CHPh_2$ **Cr2**. Using a similar procedure and molar ratios as that described for **Cr1** but with 2-methyl-4,6-dibenzhydrylaniline as the amine, **Cr2** was obtained as a green powder (0.385 g, 34%). FT-IR (KBr, cm^{-1}): $\tilde{\nu}$ = 2935 (w), 2866 (w), 1611 (s, $\nu_{C=N}$), 1552 (w), 1493 (s), 1447 (s), 1347 (m), 1246 (s), 1203 (m), 1154 (m), 1077 (m), 1031 (m), 965 (w), 915 (m), 849 (w), 790 (w), 743 (w), 698 (s). Anal. calc. for $C_{81}H_{71}Cl_3CrN_3$ (1244.83): C, 78.15; H, 5.75; N, 3.38. Found: C, 78.13; H, 5.73; N, 3.36%.

(c) R^1 = Et, R^2 = $CHPh_2$ **Cr3**. Using a similar procedure and molar ratios as that described for **Cr1** but with 2-methyl-4,6-dibenzhydrylaniline as the amine, **Cr3** was obtained as a green powder (0.344 g, 30%). FT-IR (KBr, cm^{-1}): $\tilde{\nu}$ = 2934 (w), 2871 (w), 1607 (s, $\nu_{C=N}$), 1553 (w), 1494 (m), 1447 (s), 1348 (w), 1249 (m), 1205 (m), 1154 (w), 1078 (w), 1031 (w), 965 (w), 917 (w), 846 (w), 783 (w), 743 (w), 699 (s) cm^{-1}. Anal. calc. for $C_{83}H_{75}Cl_3CrN_3$ (1272.88): C, 78.32; H, 5.94; N, 3.30. Found: C, 78.25; H, 6.01; N, 3.35%.

(d) R^1 = *i*-Pr, R^2 = $CHPh_2$ **Cr4**. Using a similar procedure and molar ratios to that described for **Cr1** but with 2-*iso*-propyl-4,6-dibenzhydrylaniline as the amine, **Cr4** was obtained as a green powder (0.480 g, 41%). FT-IR (KBr, cm^{-1}): $\tilde{\nu}$ = 2932 (w), 2868 (w), 1606 (s, $\nu_{C=N}$), 1548 (w), 1494 (m), 1448 (s), 1354 (w), 1251 (m), 1205 (m), 1154 (w), 1077 (m), 1032 (m), 962 (w), 915 (w), 846 (w), 846 (w), 743 (m), 699 (s). Anal. calc. for $C_{85}H_{79}Cl_3CrN_3$ (1300.93): C, 78.48; H, 6.12; N, 3.23. Found: C, 78.45; H, 6.26; N, 3.32%.

(e) R^1 = Cl, R^2 = $CHPh_2$ **Cr5**. Using a similar procedure and molar ratios as that described for **Cr1** but with 2-chloro-4,6-dibenzhydrylaniline as the amine, **Cr5** was obtained as a green powder (0.42

g, 36%). FT-IR (KBr, cm^{-1}): $\tilde{\nu}$ = 2935 (w), 2871 (w), 1612 (s, $\nu_{C=N}$), 1543 (w), 1494 (s), 1448 (s), 1361 (m), 1252 (s), 1203 (m), 1151 (m), 1079 (m), 1042 (m), 962 (w), 920 (m), 849 (w), 758 (w), 743 (w), 699 (s). Anal. calc. for $C_{85}H_{79}Cl_2FeN_3$ (1269.3)**:** $C_{79}H_{65}Cl_5CrN_3$ (1285.66): C, 73.80; H, 5.10; N, 3.27**.** Found C, 73.60; H, 5.14; N, 3.30%.

(f) R^1 = F, R^2 = $CHPh_2$ **Cr6**. Using a similar procedure and molar ratios as that described for **Cr1** but with 2-flouro-4,6-dibenzhydrylaniline as the amine, **Cr6** was obtained as a green powder (0.91 g, 80%). FT-IR (KBr, cm^{-1}): $\tilde{\nu}$ = 2935 (w), 2871 (w), 1612 (s, $\nu_{C=N}$), 1543 (w), 1494 (s), 1448 (s), 1361 (w), 1252 (m), 1203 (m), 1151 (w), 1079 (w), 1042 (w), 920 (w), 894 (w), 849 (w), 806 (w), 743 (w), 699 (s). Anal. calc. for $C_{85}H_{79}Cl_2FeN_3$ (1269.3)**:** $C_{79}H_{65}Cl_3CrF_2N_3$ (1252.75): C, 75.74; H, 5.23; N, 3.35. Found C, 75.63; H, 5.28; N, 3.30%.

Ethylene polymerization at P_{C2H4} = 5 or 10 atm

The polymerization at 5 or 10 atm C_2H_4 was performed in a stainless steel autoclave (250 mL) equipped with an ethylene pressure control system, a mechanical stirrer and a temperature controller. The autoclave was evacuated and backfilled with ethylene three times. When the required temperature was reached, the precatalyst (5 μmol) was dissolved in toluene (30 mL) in a Schlenk tube and then transferred by syringe to the autoclave, maintained under an ethylene atmosphere (*ca*. 1 atm). Toluene (30 mL) and the required amount of co-catalyst were then successively introduced followed by additional toluene taking the total volume of solvent to 100 mL. The autoclave was immediately pressurized with 5 or 10 atm C_2H_4 and the stirring commenced. After the required reaction time, the reactor was cooled with a water bath and the excess ethylene vented. Following quenching of the reaction with 10% hydrochloric acid in ethanol, the polymer was collected and washed with ethanol and dried under reduced pressure at 50 °C and weighed.

Ethylene polymerization at P_{C2H4} = 1 atm

The polymerization at 1 atm C_2H_4 was carried out in a Schlenk tube. Under an atmosphere of ethylene (*ca.* 1 atm), **Cr1** (4.0 μmol) was added followed by toluene (30 mL) and then the required amount of co-catalyst introduced by syringe. The resulting solution was then stirred at 30 ºC under an ethylene atmosphere (1 atm). After 30 min, the solution was quenched with 10% hydrochloric acid in ethanol. The polymer was washed with ethanol, dried under reduced pressure at 40 °C and then weighed.

X-ray Crystallographic Studies

The single crystal X-ray diffraction study of **Cr1** was carried out on a Rigaku sealed Tube CCD (Saturn 724+) diffractometer with graphite-monochromated Mo-K_α radiation (λ = 0.71073 Å) at 173(2) K; cell parameters were obtained by global refinement of the positions of all collected reflections. Intensities were corrected for Lorentz and polarization effects and empirical absorption. The structures were solved by direct methods and refined by full-matrix least squares on F^2. All non-hydrogen atoms were placed in calculated positions. Structural solution and refinement were performed by using the SHELXTL-97 package [59,60]. The free solvent molecules present within the crystal structure were removed by using the SQUEEZE option of the crystallographic program PLATON [60]. Details of the X-ray refinements are provided in Table 1.

<Table 1>

Results and discussion

The template reaction of the diketone α,α′-dioxo-2,3:5,6-bis(pentamethylene)pyridine with four equivalents of 2-R^1-4-R^2-6-$(CHPh_2)C_6H_2NH_2$ (R^1 = Me, R^2 = Me; R^1 = Me, R^2 = $CHPh_2$; R^1 = Et, R^2 = $CHPh_2$; R^1 = *i*-Pr, R^2 = $CHPh_2$; R^1 = Cl, R^2 = $CHPh_2$; R^1 = F, R^2 = $CHPh_2$) in the presence of $CrCl_3(THF)_3$ gave, on work-up, [2,3:5,6-$\{C_4H_8C(N(2\text{-}R^1\text{-}4\text{-}R^2\text{-}6\text{-}(CHPh_2)C_6H_2))\}_2C_5HN]CrCl_3$ (R^1 = R^2 = Me **Cr1**, R^1 = Me, R^2 = $CHPh_2$ **Cr2**, R^1 = Et, R^2 = $CHPh_2$ **Cr3**, R^1 = *i*-Pr, R^2 = $CHPh_2$ **Cr4**, R^1 = Cl, R^2 = $CHPh_2$ **Cr5**, R^1 = F, R^2 = $CHPh_2$ **Cr6**), in moderate to good yield (30 - 81%) (Scheme 1). The free ligands were not amenable to isolation and so the above template approach was undertaken to afford the complexes in one step; similar one pot approaches have been employed elsewhere [51,61-67]. All the chromium(III) complexes were air stable green solids that have been characterized by infra-red spectroscopy and by microanalysis. In addition, the structure of **Cr1** has been determined by single crystal X-ray diffraction.

<Scheme 1>

Single crystals of **Cr1** suitable for the X-ray determination were grown by slow diffusion of diethyl ether into a dichloromethane solution of the corresponding complex at ambient temperature. A view of **Cr1** is shown in Figure 1; selected bond distances and angles are collected in Table 2. The structure of **Cr1** consists of a single chromium center surrounded by three *mer*-configured nitrogen donors belonging to the *N,N,N*-chelating α,α'-bis(arylimino)-2,3:5,6-bis(pentamethylene)pyridine ligand and three chlorides to complete a six-coordinate geometry

which can be best described as distorted octahedral; similar structural features have been noted in (**E**$_{2,6\text{-Me2Ph}}$)$CrCl_3$ and (**E**$_{2,4,6\text{-Me3Ph}}$)$CrCl_3$ (Chart 1) [51]. The central Cr-N_{py} bond distance [Cr1-N1 2.007(2) Å)] is shorter when compared to the exterior Cr–N_{imine} bond lengths [Cr1–N2 2.127(2) Å; Cr–N3 2.126(2) Å], highlighting the more effective coordination of the pyridine unit. Furthermore, the Cr–N_{py} distance when compared with that in **A** (range: 1.981(3)-2.001(3) Å) [31-34], **B** (1.985(6) Å) [48] and **C** (1.985(4) Å) [49] is slightly longer but compares favorably to that seen in **D** (2.015(3) Å) [50] and **E** (2.004(2) Å, 2.003(3) Å) [51]. Within the tridentate ligand the saturated C2-C3-C4-C5 and C9-C10-C11-C12 sections of the two fused rings are puckered with the result that both fold towards Cl1 so as to adopt a mutually *cis* configuration. The Cr-Cl bond lengths show some differences with the chloride *trans* to pyridine the shortest [Cr(1)-Cl(2) 2.2923(8) Å]. On the other hand, the longer *trans*-chlorides are uneven with the Cr(1)-Cl(1) bond (2.3352(8) Å) noticeably longer than Cr(1)-Cl(3) (2.2954(8) Å). Meanwhile, the *N*-aryl groups show some variation in their inclination with respect to their neighboring imine vectors (85.1° and 69.4°), which is likely due to the steric properties of the *ortho*-benzhydryl groups which sit above and below the plane of the central pyridine ring. There are no intermolecular contacts of note.

All six complexes showed strong peaks around 1600 cm^{-1} in their IR spectra which can be attributed to the C=N stretching vibrations belonging to coordinated imines [48-51]. Furthermore, the micro-analytical data for **Cr1** – **Cr6** were in full agreement with the elemental compositions of general formula $LCrCl_3$.

<Figure 1>

<Table 2>

Ethylene polymerization evaluation

(a) *Co-catalyst screen.* Before a full catalytic evaluation of all the new chromium precatalysts was performed, **Cr1** was subjected to a preliminary study to determine the two most effective co-catalysts to promote the polymerization. In particular, four different alkylaluminum co-catalysts namely, modified methylaluminoxane (MMAO), methylaluminoxane (MAO), diethylaluminum chloride (Et_2AlCl) and ethylaluminum sesquichloride (EASC), were initially evaluated. Typically, the polymerizations were performed in toluene under 10 atm C_2H_4 at 30 °C over a 30 minute time period (Table 3). All the polymers were characterized by gel permeation chromatography (GPC) and differential scanning calorimetry (DSC). In all runs gas chromatography (GC) was performed to check for any oligomeric fractions generated during the runs.

In each instance polymers were generated and no evidence for shorter chain oligomers could be detected. Examination of the results reveal that the catalytic activity for **Cr1**, as a function of the

co-catalyst, falls in the order: MMAO > MAO > Et_2AlCl > EASC. Indeed, previous studies of structurally related *N,N,N*-bound chromium(III) complexes, have also revealed MAO and MMAO to be the most effective co-catalysts to promote ethylene polymerization [33,48-51]. On the basis of the higher activities observed, MMAO and MAO were chosen for more in-depth catalytic investigations discussed below. It is worthy of note that catalysts derived from Et_2AlCl or EASC activation, although less active, produced the polymers exhibiting the highest molecular weight of the four runs (entries 3 and 4, Table 3).

<Table 3>

(b) *Precatalyst evaluation using MMAO*. To ascertain the optimal polymerization conditions using MMAO, the run temperature, the Al:Cr molar ratio and run time were all systematically varied using **Cr1** as the test precatalyst; the results of the runs are collected in Table 4. Firstly, with the Al:Cr molar ratio set at 2000, the reaction temperature was increased from 20 to 60 °C leading to a peak in activity of 9.29×10^5 g(PE) mol^{-1}(Cr) h^{-1} being recorded at 20 °C (entries 1 – 5, Table 4). Above 20 ºC, the activity steadily decreased reaching its lowest value of 0.75×10^5 g(PE) mol^{-1}(Cr) h^{-1} at 60 ºC (entry 5, Table 4) which can be accredited to the onset of catalyst deactivation [48,62,65-67]. In terms of molecular weight, the corresponding polymers followed a similar downward trend (M_w: from 106.6 to 21.9 kg mol^{-1}) on increasing temperature which can be ascribed to chain transfer occurring faster than chain propagation under these conditions [43,50,68-69]. As a general observation, the molecular weight distributions for the polymers were narrow to broad (M_w/M_n = 2.8 – 10.3) (Figure 2a).

With the temperature fixed at 20 ºC, the Al:Cr ratio was varied between 1000 and 3000 leading to a maximum activity attained of 12.81×10^5 g(PE) mol^{-1}(Cr) h^{-1} at 1500 (entry 8, Table 4). Above 1500, the activity gradually decreased reaching a minimum value of 7.52×10^5 g(PE) mol^{-1}(Cr) h^{-1} at 3000 (entry 11, Table 4). With regard to the molecular weight of the polyethylene, this was found to steadily decrease as the Al:Cr ratio was increased dropping from 207.3 kg mol^{-1} with 1000 equivalents to 60.4 kg mol^{-1} with 3000 equivalents (Figure 2b); a narrower range in molecular weight distributions (M_w/M_n range: 2.3 – 6.2) was in this case observed.

By performing the polymerizations over intervals of 5, 15, 30, 45 and 60 minutes, with the temperature maintained at 20 °C and the Al:Cr molar ratio at 1500, the activity reached a peak of 12.81×10^5 g (PE) mol^{-1} (Cr) h^{-1} after 30 minutes, Notably, after 45 minutes a 33% loss in activity was observed while after 60 minutes this percentage had increased to only 50% with a catalytic

activity of 6.50 g (PE) mol^{-1}(Cr) h^{-1} noted (entry 15, Table 4). These results highlight both the slow induction period needed to form the active species and the gradual deactivation of the catalyst over time [50,67]. In terms of the molecular weight, the longer reaction time was accompanied by an increase in the value of M_w from 104.8 kg mol^{-1} after 5 minutes to 172.8 kg mol^{-1} after 60 minutes (Figure 2c).

The effect of ethylene pressure was also found to be significant with the activity dramatically lowering as the pressure was reduced from 10 to 1 atm (entries 8, 16 and 17, Table 4); lower molecular weight polyethylenes were also observed. These findings are consistent with chain propagation decreasing as the ethylene pressure was reduced.

To investigate the influence of structural variations made to the precatalyst on catalyst performance and polymer properties, **Cr2** - **Cr6** were also investigated using the optimal conditions established for **Cr1**/MMAO [Al:Cr = 1500, temperature = 20 ºC, reaction time = 30 minutes]. Reasonable to good activities of between 1.95 - 18.33 × 10^5 g (PE) mol^{-1}(Cr) h^{-1} were observed for all five precatalysts and when put alongside **Cr1** fall in the order (entries 8, 18 - 22, Table 4): **Cr6** (2-fluoro-4,6-dibenzhydryl) > **Cr5** (2-chloro-4,6-dibenzhydryl) > **Cr1** (2,4-methyl-6-dibenzhydryl) > **Cr2** (2-methyl-4,6-dibenzhydryl) > **Cr3** (2-ethyl-4,6-dibenzhydryl) > **Cr4** (2-*iso*-propyl-4,6-dibenzhydryl). Notably, **Cr6** and **Cr5** containing the *ortho*-halide substituents F and Cl, respectively, displayed the highest activities which likely reflects the electron withdrawing properties of these ligands though steric factors may also be influential. On the other hand, the steric properties exerted by the *ortho*-alkyl substituents are clearer to identify with the least bulky **Cr1** (R^1 = Me) and **Cr2** (R^1 = Me) more active than **Cr3** (R^1 = Et) and isopropyl **Cr4** (**R^1** = i-Pr). These findings can be attributed to the more sterically encumbered substituent impeding the coordination and insertion of the ethylene monomer [66,67]. Furthermore, the nature of the 4-R^2 group also affects the catalytic activity as revealed by 4-Me **Cr1** being more active than 4-$CHPh_2$ **Cr2**, which suggests electronic properties of the *para* group also play a role. With respect to the molecular weight, a remarkably wide range in values were observed [M_w range: 2.17 - 300.4 kg mol^{-1}] with the most bulky **Cr3** and **Cr4** generating polymer at the top end while the *ortho*-halides **Cr5** and **Cr6** at the bottom end.

For purposes of comparison the catalytic activity of **Cr1** – **Cr6**/MMAO as well as the molecular weights for the resulting polymers are presented alongside those obtained using $\mathbf{E}_{2,4,6\text{-}Me3Ph}$/MMAO (Chart 1, Ar = 2,4,6-Me_3Ph); all determined under comparable reaction conditions (Figure 3) [51]. Several points emerge from examination of the figure. Firstly, the catalytic activity of $\mathbf{E}_{2,4,6\text{-}Me3Ph}$/MMAO significantly exceeds even the most active system disclosed in this study (i.e.,

Cr6/MMAO: 1.83 × 10^6 g(PE) mol^{-1}(Cr) h^{-1}). Indeed, a wide range of **E**-type precatalysts (Chart 1) have been reported with activities typically falling in the range 6.8 - 14.6 × 10^6 g(PE) mol^{-1}(Cr) h^{-1}, the precise value depending on the N-aryl substitution pattern (Ar = 2,6-Me_2Ph, 2,6-Et_2Ph, 2,6-$^iPr_2$Ph, 2,4,6-Me_3Ph, 2,6-Et_2-4-MePh) [51]. Secondly, it is clear that the molecular weight of the polymer obtained using the *ortho*-benzhydryl systems **Cr1** – **Cr5** developed herein is significantly higher than that seen with $\mathbf{E}_{Me3Ph}$/MMAO. Conversely, **Cr6**/MMAO generated polymer of similar low molecular weight. It would appear that the choice of the benzhydryl/R^1 *ortho*-pairing is crucial to performance characteristics of the current chromium catalysts. Nevertheless, the presence of the sterically hindered benzhydryl group does in most cases have the effect of inhibiting chain transfer leading to more efficient propagation and in-turn higher molecular weight.

It is worth noting that the **E**-type precatalysts, when activated with Et_2AlCl, displayed relatively lower catalytic activities of between 1.73 - 3.00 × 10^5 g (PE) mol^{-1} (Cr) h^{-1} with molecular weights as high as 630.3 - 1189.6 kg mol^{-1} [51]. By way of comparison, a similar low activity/high molecular weight trend was observed in our preliminary investigation using Et_2AlCl as co-catalyst (Table 3).

<Table 4>

<Figure 2>

<Figure 3>

(c) *Precatalyst evaluation using MAO.* To complement the study undertaken with MMAO, we also examined the performance of **Cr1** using MAO as co-catalyst. As before, the first stage of the catalytic optimization focused on the effect of temperature (entries 1 - 5, Table 5). The highest activity was achieved at 30 ºC (12.85 × 10^5 g (PE) mol^{-1} (Cr) h^{-1}) above which the activity steadily reduced until at 60 ºC the activity had dropped by almost six-fold. At the same time, the molecular weight of the polymer decreased with increased temperature from 48.0 to 33.6 kg mol^{-1} (see Figure 4a).

With the temperature maintained at 30 ºC, the effect of varying the Al:Cr molar ratio from 1000 to 3000 was studied. A peak in activity of 13.70 × 10^5 g (PE) mol^{-1} (Cr) h^{-1} was identified with an Al:Cr ratio of 2250 (entries 2, 6-11, Table 5). As with the MMAO investigation, the molecular weight steadily dropped in this case from 140.5 - 34.6 kg mol^{-1} as the molar ratio of Al:Cr increased in agreement with increased chain transfer from the active chromium species to aluminum (see Figure 4b) [63,64].

To explore the lifetime of the catalyst, the polymerization runs were performed over different time intervals with the highest activity of 13.70 × 10^5 g(PE) mol^{-1}(Cr) h^{-1} being observed after 30

minutes (entry 9, Table 5); a similar time dependence was observed with MMAO. The catalyst displayed good stability and even at the 60 minute mark the activity had lowered to only 8.70×10^5 g(PE) mol^{-1}(Cr) h^{-1} (entries 9, 12 - 15, Table 5) (Figure 4c). On the other hand, and as noted with MMAO, the catalyst activity of **Cr1**/MAO was also found to drop markedly on reducing the ethylene pressure for 10 to 5 to 1 atm, while the molecular weight of the material remained comparable at all these pressures.

With the optimized conditions established for **Cr1**/MAO [Al:Cr = 2250, temperature = 30 ºC, reaction time = 30 minutes], the remaining five precatalysts were also screened similarly. Under these conditions **Cr2** – **Cr6** all displayed good activities in the range $3.30 – 17.15 \times 10^5$ g(PE) mol^{-1}(Cr) h^{-1}, which compares with $1.95 – 18.33 \times 10^5$ g(PE) mol^{-1}(Cr) h^{-1} obtained using MMAO. In terms of the precatalyst structure, similar trends to those seen with MMAO were observed with the highest activity observed with the *ortho*-chloride **Cr5** and *ortho*-fluoride **Cr6** while the *ortho*-alkyl precatalyts (**Cr1** - **Cr4**) displayed lower activity (entries 9, 18 - 22, Table 5). By contrast, the most sterically bulky catalyst **Cr4** produced the highest molecular weight polyethylene (270 g mol^{-1}) with the broadest molecular weight distribution (M_w/M_n = 4.7).

<Table 5>

<Figure 4>

(d) *Structural properties of the polyethylenes.* As a common feature to both the MMAO and MAO investigations, high melting temperatures (T_m) were a feature of the polymers obtained using **Cr1** – **Cr5** with the values typically between 130.4 - 134.1 ºC. By contrast for **Cr6**, with either MMAO or MAO, the T_m's were around 123 ºC which likely reflects the lower molecular weight polyethylene generated. Indeed, the melting temperature of the low molecular weight polymer produced by $\mathbf{E}_{2,4,6\text{-Me3Ph}}$/MMAO resembles that obtained with **Cr6**/MMAO [51]. Nevertheless, all these melt temperatures obtained suggest that the polymers adopt linear structures.

To provide further evidence for the linearity of the polymers, representative samples synthesized using **Cr1**/MMAO at 20 ºC, (entry 8, Table 4) and **Cr1**/MAO at 30 ºC (entry 9, Table 5) were investigated by ^{13}C NMR spectroscopy (recorded in 1,1,2,2-tetrachloroethane-d_2 at 135 ºC). In each case the spectra revealed an intense peak centered at δ 30.0 corresponding the -$(CH_2)_n$- repeat unit in a linear polymer. On closer inspection of the aliphatic region, additional peaks at δ 32.11, 22.80 and 14.12 (peaks 1, 2 and 3 in Figure 5) can be attributed to *n*-propyl end-groups [65,67,70]. No evidence of downfield peaks corresponding to an unsaturated chain end could be detected for either sample. These findings would suggest that termination of these polymerizations occurs by chain transfer from chromium to aluminum leading to fully saturated polymers [65].

<Figure 5>

Conclusions

Six examples of chromium complexes bearing *ortho*-benzhydryl-substituted α,α′-bis(arylimino)-2,3:5,6-bis(pentamethylene)pyridines, that differ in the steric/electronic properties of the second *ortho*-R^1 group (halide *vs.* alkyl) as well as the *para*-R^2 substituent (Me *vs.* $CHPh_2$), have been successfully synthesized by using a one-pot approach and fully characterized. On activation with either MMAO or MAO, all precatalysts showed good activity for ethylene polymerization with those containing *ortho*-halide substituents (**Cr5** (Cl), **Cr6** (F)) notably more active than their *ortho*-alkyl counterparts (**Cr1** – **Cr4**). Moreover, the nature of *ortho*-R^1 substituent had a pronounced effect on the molecular weight of the polymers with wax-like materials obtained with fluoride-containing **Cr6** (M_w: 2.17 – 2.29 kg mol^{-1}), while isopropyl **Cr4** formed high molecular weight linear polyethylene (M_w: 270.4 – 300.4 kg mol^{-1}). By comparison with the benzhydryl-free catalyst, $\mathbf{E}_{2,4,6\text{-Me3Ph}}$/MMAO (Chart 1), **Cr1** – **Cr5** proved less active but produced noticeably higher molecular weight polymer. End-group analysis also reveals the importance of chain transfer to aluminum as the termination pathway in these polymerizations.

Conflicts of interest

There are no conflicts to declare.

Acknowledgements

This work was supported by the National Natural Science Foundation of China (Nos. 21871275 and 51861145303). CB is grateful to the CAS-TWAS President's fellowship. GAS thanks the Chinese Academy of Sciences for a President's International Fellowship for Visiting Scientists.

Supplementary data

X-ray crystallographic data in CIF for CCDC 1880230 (**Cr1**) available free of charge from the Cambridge Crystallographic Data Centre. Supplementary data related to this article can be found at https://doi.org/....

References

1. V. C. Gibson, S. K. Spitzmesser, Advances in non-metallocene olefin polymerization catalysis, Chem. Rev. 103 (2003) 283–315.
2. T. Agapie, Selective ethylene oligomerization: Recent advances in chromium catalysis and

mechanistic investigations, Coord. Chem. Rev. 255 (2011) 861–880.
3. J. T. Dixon, M. J. Green, F. M. Hess, D. H. Morgan, Advances in selective ethylene trimerisation – a critical overview, J. Organomet. Chem. 689 (2004) 3641–3668.
4. D. F. Wass, Chromium-catalysed ethene trimerisation and tetramerisation—breaking the rules in olefin oligomerisation, Dalton Trans. (2007) 816–819.
5. D. S. Guinness, Olefin oligomerization via metallacycles: Dimerization, trimerization, tetramerization, and beyond, Chem. Rev. 111 (2011) 2321–2341.
6. K. A. Alferov, G. P. Belov, Y. Meng, Chromium catalysts for selective ethylene oligomerization to 1-hexene and 1-octene: Recent results, Appl. Cat. A: Gen. 542 (2017) 71–124.
7. A. Otero, J. Fernández-Baeza, A. Lara-Sánchez, L. F. Sánchez-Barba, Metal complexes with heteroscorpionate ligands based on the bis(pyrazol-1-yl)methane moiety: Catalytic chemistry, Coord. Chem. Rev. 257 (2013) 1806–1868.
8. C. Fliedel, A. Ghiosolfi, P. Braunstein, Functional short-bite ligands: Synthesis, coordination chemistry, and applications of N - functionalized bis(diaryl/dialkylphosphino)amine-type ligands, Chem. Rev. 116 (2016) 9237–9304.
9. P. W. N. M. van Leeuwen, N. D. Clément, M. J.-L. Tschan, New processes for the selective production of 1-octene, Coord. Chem. Rev. 255 (2011) 1499−1517.
10. D. Peng, X. Yan, C. Yu, S. Zhang, X. Li, Transition metal complexes bearing tridentate ligands for precise olefin polymerization, Polym. Chem. 7 (2016) 2601−2634.
11. K. H. Theopold, Homogeneous chromium catalysts for olefin polymerization, Eur. J. Inorg. Chem. (1998) 15–24.
12. C. Bariashir, C. Huang, G. A. Solan, W.-H. Sun, Recent advances in homogeneous chromium catalyst design for ethylene tri-, tetra-, oligo- and polymerization, Coord. Chem. Rev. 385 (2019) 208-229
13. M. P. McDaniel, A review of the Phillips supported chromium catalyst and its commercial use for ethylene polymerization, advances in catalysis, Elsevier Academic Press Inc. 53 (2010) pp. 123–606 ISBN:978-0-12-380852-3.
14. W. K. Reagan, Phillips Petroleum Company, Process for olefin polymerization. EP Pat, (1991) 0 417 477.

15. W. K. Reagan, J. W. Freeman, B. K. Conroy, T. M. Pettijohn, E. A. Benham, Phillips Petroleum Company, Process for the preparation of a catalyst for olefin polymerization, EP Pat, (1994) 0608447.
16. R. D. Knudsen, J. W. Freeman, M. E. Lashier, Phillips Petroleum Company, Olefin Production. US Pat., (1996) 5563312.
17. J. W. Freeman, J. L. Buster and R. D. Knudsen, Phillips Petroleum Company, Olefin Production. US Pat., (1999) 5856257.
18. W. K. Reagan, J. W. Freeman, B. K. Conroy, T. M. Pettijohn, E. A. Benham, Phillips Petroleum Company, Process for olefin polymerization. US Pat., (1995) 5451645.
19. D. S. McGuinness, P. Wasserscheid, W. Keim, D. Morgan, J. T. Dixon, A. Bollmann, H. Maumela, F. Hess, U. Englert, First Cr(III)-SNS complexes and their use as highly efficient catalysts for the trimerization of ethylene to 1-hexene, J. Am. Chem. Soc. 125 (2003) 5272-5273.
20. J. Zhang, P. Braunstein, T. S. A. Hor, Highly selective chromium(III) ethylene trimerization catalysts with [NON] and [NSN] heteroscorpionate ligands, Organometallics 27 (2008) 4277–4279.
21. D. S. McGuinness, P. Wasserchied, W. Keim, C. Hu, U. Englert, J.T. Dixon, C. Grove, Novel Cr-PNP complexes as catalysts for the trimerisation of ethylene, Chem. Commun. (2003) 334–335.
22. D. S. McGuinness, P. Wasserchied, D. H. Morgan, J. T. Dixon, Ethylene trimerization with mixed-donor ligand (N,P,S) chromium complexes: Effect of ligand structure on activity and selectivity, Organometallics 24 (2005) 552–556.
23. K. Blann, A. Bollmann, J. T. Dixon, F. M. Hess, E. Killian, H. Maumela, D. H. Morgan, A. Neveling, S. Otto, M. J. Overett, New insight into the role of the metal oxidation state in controlling the selectivity of the Cr-(SNS) ethylene trimerization catalyst, Chem. Commun. 2005, 620–621.
24. D. S. McGuinness, D. B. Brown, R. T. Tooze, F. M. Hess, J. T. Dixon, A. M. Z. Slawn, Ethylene trimerization with Cr-PNP and Cr-SNS complexes: Effect of ligand structure, metal oxidation state, and role of activator on catalysis, Organometallics 25 (2006) 3605–3610.
25. A. Bollmann, K. Blann, J. T. Dixon, F. M. Hess, E. Killian, H. Maumela, D. S. McGuinness, D. H. Morgan, A. Nveling, S. Otto, M. Overett, A. M. Z. Slawin, P. Wasserscheid, S.

Kuhlmann, Ethylene tetramerization: A new route to produce 1-octene in exceptionally high selectivities, J. Am. Chem. Soc.126 (2004) 14712–14713.

26. A. J. Rucklidge, D. S. McGuinness, R. P. Tooze, A. M. Z. Slawin, J. D. A. Pelletier, M. J. Hanton, P. B. Webb, Ethylene tetramerization with cationic chromium(I) complexes, Organometallics 26 (2007) 2782–2787.
27. M. J. Overett, K. Blann, A. Bollmann, J. T. Dixon, F. Hess, E. Killian, H. Maumela, D. H. Morgan, A. Neveling, S. Otto, Ethylene trimerisation and tetramerisation catalysts with polar substituted diphosphinoamine ligands, Chem. Commun. (2005) 622–624.
28. A. Jabri, P. Crewdson, S. Gambarotta, I. Korobkov, R. Duchateau, Isolation of a cationic chromium(II) species in a catalytic system for ethylene tri- and tetramerization, Organometallics 25 (2006) 715–718.
29. R. D. Köhn, M. Haufe, S. Mihan, D. Lilge, Triazacyclohexane complexes of chromium as highly active homogeneous model systems for the Phillips catalyst, Chem. Commun. (2000) 1927–1928.
30. R. D. Köhn, M. Haufe, G. Kociok-Köhn, S. Grimm, P. Wasserscheid, W. Keim, Selective trimerization of α-olefins with triazacyclohexane complexes of chromium as catalysts, Angew. Chem. Int. Ed. 39 (2000) 4337–4339.
31. M. A. Esteruelas, A. M. López, L. Méndez, M. Oliván, E. Oñate, Preparation, structure, and ethylene polymerization behavior of bis(imino)pyridyl chromium(III) complexes, Organometallics 22 (2003) 395-406.
32. N. V. Semikolenova, V. A. Zakharov, L. G. Echevskaja, M. A. Matsko, K. P. Bryliakov, E. P. Talsi, Homogeneous catalysts for ethylene polymerization based on bis(imino)pyridine complexes of iron, cobalt, vanadium and chromium, Catal. Today. 144 (2009) 334–340.
33. Y. Nakayama, K. Sogo, H. Yasuda, T. Shiono, Unique catalytic behavior of chromium complexes having halogenated bis(imino)pyridine ligands for ethylene polymerization, J. Polym. Sci. Part A: Polym. Chem. 43 (2005) 3368–3376.
34. B. L. Small, M. J. Carney, D. M. Holman, C. E. O'Rourke, J. A. Halfen, New chromium complexes for ethylene oligomerization: Extended use of tridentate ligands in metal-catalyzed olefin polymerization, Macromolecules 37 (2004) 4375–4386.
35. M. J. Carney, N. J. Robertson, J. A. Halfen, L. N. Zakharov, A. L. Rheingold, Octahedral chromium(III) complexes supported by bis(2-pyridylmethyl)amines: Ligand influence on coordination geometry and ethylene polymerization activity, Organometallics 23 (2004) 6184–6190.

36. M. A. Esteruelas, A. M. López, L. Méndez, M. Oliván, E. Oñate, Synthesis, x-ray structure, and polymerisation activity of a bis(oxazolinyl)pyridine chromium(III) complex, New J. Chem. 26 (2002) 1542–1544.
37. D. Wang, S. Liu, Y. Zheng, W.-H. Sun, C. Redshaw, 2-Benzimidazolyl-N-phenylquinoline-8-carboxamide chromium(III) trichlorides: Synthesis and application for ethylene oligomerization and polymerization, Organometallics 30 (2011) 3001–3009.
38. A. E. Ceniceros-Gómez, N. Barba-Behrens, M. E. Quiroz-Castro, S. Bernès, H. Nöth, S. E. Castillo-Blum, Synthesis, X-ray and spectroscopic characterisation of chromium(III) coordination compounds with benzimidazolic ligands, Polyhedron 19 (2000) 1821–1827.
39. J. Zhang, A. Li, T. S. A. Hor, Crystallographic revelation of the role of $AlMe_3$ (in MAO) in Cr[NNN] pyrazolyl catalyzed ethylene trimerization, Organometallics 28 (2009) 2935–2937.
40. J. Hurtao, D. M-L. Carey, A. Muñoz-Castro, R. Arratia-Pérez, R. Quijada, G. Wu, R. Rojas, M. Valderrama, Chromium(III) complexes with terdentate 2,6-bis(azolylmethyl)pyridine ligands: Synthesis, structures and ethylene polymerization behavior, J. Organomet. Chem. 694 (2009) 2636–2641.
41. M. A. Esteruelas, A. M. López, L. Méndez, M. Oliván, E. Oñate, Synthesis, x-ray structure, and polymerisation activity of a bis(oxazolinyl)pyridine chromium(III) complex, New J. Chem. 26 (2002) 1542–1544.
42. W. Zhang, W.-H. Sun, S. Zhang, J. Hou, K. Wedeking, S. Schultz, R. Frölich, H. Song, Synthesis, characterization, and ethylene oligomerization and polymerization of [2,6-Bis(2-benzimidazolyl)pyridyl]chromium chlorides, Organometallics 25 (2006) 1961–1969.
43. L. Xiao, M. Zhang, W.-H. Sun, Synthesis, characterization and ethylene oligomerization and polymerization of 2-(1H-2-benzimidazolyl)-6-(1-(arylimino)ethyl)pyridylchromium chlorides, Polyhedron 29 (2010) 142–147.
44. Y. Chen, W. Zuo, P. Hao, S. Zhang, K. Gao W.-H. Sun, Chromium(III) complexes ligated by 2-(1-isopropyl-2-benzimidazolyl)-6-(1-(arylimino)ethyl)pyridines: Synthesis, characterization and their ethylene oligomerization and polymerization, J. Organomet. Chem. 693 (2008) 750–762.
45. S. A. Amolegbe, M. Asma, M. Zhang, G. Li, W.-H. Sun, Synthesis, characterization, and ethylene oligomerization and polymerization by 2-quinoxalinyl-6-iminopyridine chromium chlorides, Aust. J. Chem. 61 (2008) 397–403.

46. R. Gao, T. Liang, F. Wang, W.-H. Sun, Chromium(III) complexes bearing 2-benzoxazolyl-6-arylimino-pyridines: Synthesis and their ethylene reactivity, J. Organomet. Chem. 694 (2009) 3701–3707.
47. Z. Wang, G. A. Solan, W. Zhang, W.-H. Sun, Carbocyclic-fused N,N,N-pincer ligands as ring-strain adjustable supports for iron and cobalt catalysts in ethylene oligo-/polymerization, Coord. Chem. Rev. 363 (2018) 92–108.
48. Y. Zhang, C. Huang, X. Hao, X. Hu, W.-H. Sun, Accessing highly linear polyethylenes by 2-(1-aryliminoethyl)-7-arylimino-6,6-dimethylcyclopenta[*b*]pyridylchromium(III) chlorides, RSC Adv. 6 (2016) 91401–91408.
49. C. Huang, Y. Zhang, G. A. Solan, Y. Ma, X. Hu, Y. Sun, W.-H. Sun, Vinyl-polyethylene waxes with narrow dispersity obtained by using a thermally robust [bis(imino)trihydroquinolyl]chromium catalyst, Eur. J. Inorg. Chem. (2017) 4158–4166.
50. C. Huang, Y. Huang, Y. Ma, G. A. Solan, Y. Sun, X. Hu, W.-H. Sun, Cycloheptyl-fused N,N,N'-chromium catalysts with selectivity for vinyl-terminated polyethylene waxes: Thermal optimization and polymer functionalization, Dalton Trans. 47 (2018) 13487–13497.
51. C. Huang, S. Du, G. A. Solan, Y. Sun, W.-H. Sun, From polyethylene waxes to HDPE using an α,α'-bis(arylimino)-2,3:5,6-bis(pentamethylene)pyridyl-chromium(III) chloride pre-catalyst in ethylene polymerisation, Dalton Trans. 46 (2017) 6948–6957.
52. Z. Wang, Q. Liu, G. A. Solan, W.-H. Sun, Recent advances in Ni-mediated ethylene chain growth: N_{imine}-donor ligand effects on catalytic activity, thermal stability and oligo-/polymer structure, Coord. Chem. Rev. 350 (2017) 68–83.
53. R. P. Thummel, Y. Jahng, Polyaza cavity shaped molecules. Annelated derivatives of 2,2':6',2''-terpyridine, J. Org. Chem. 50 (1985) 2407–2412.
54. S. Du, W. Zhang, E. Yue, F. Huang, T. Liang, W.-H. Sun, α,α′-Bis(arylimino)-2,3:5,6-bis(pentamethylene)pyridylcobalt chlorides: Synthesis, characterization, and ethylene polymerization behavior, Eur. J. Inorg. Chem. (2016) 1748–1755.
55. S. Meiries, K. Speck, B. D. Cordes, A. M. Z. Slawin, S. P. Nolan, [Pd(IPr*OMe)(acac)Cl]: Tuning the N‑heterocyclic carbene in catalytic C−N bond formation, Organometallics 32 (2013) 330–339.
56. P. Shaw, A. R. Kennedy, D. J. Nelson, Synthesis and characterisation of an N-heterocyclic carbene with spatially-defined steric impact, Dalton Trans. 45 (2016) 11772–11780.

57. J. H. So, P. Boudjouk, A convenient synthesis of solvated and unsolvated anhydrous metal chlorides via dehydration of metal chloride hydrates with trimethylchlorosilane, Inorg. Chem. 29 (1990) 1592–1593.
58. J. Y. Jeon, J. H. Park, D. S. Park, S. Y. Park, C. S. Lee, M. J. Go, J. Lee, B. Y. Lee, Concerning the chromium precursor $CrCl_3(THF)_3$, Inorg. Chem. Commun. 44 (2014) 148–150.
59. G. M. Sheldrick, SHELXT-Integrated space-group and crystal-structure determination, Acta Cryst, Acta Cryst. A71 (2015) 3–8.
60. G. M. Sheldrick, Crystal structure refinement with SHELXL, *Acta Cryst*. C71 (2015) 3–8.
61. V. K. Appukuttan, Y. Liu, B. C. Son, C.-S. Ha, H. Suh, I. Kim, Iron and cobalt complexes of 2,3,7,8-tetrahydroacridine-4,-5(1H,6H)-diimine sterically modulated by substituted aryl rings for the selective oligomerization to polymerization of ethylene, Organometallics 30 (2011) 2285–2294.
62. F. Huang, W. Zhang, Y. Sun, X. Hu, G. A. Solan, W.-H. Sun, Thermally stable and highly active cobalt precatalysts for vinyl-polyethylenes with narrow polydispersities: integrating fused-ring and imino-carbon protection into ligand design, New J. Chem. 40 (2016) 8012–8023.
63. Y. Zhang, H. Suo, F. Huang, T. Liang, X. Hu, W.-H. Sun, Thermo-stable 2-(arylimino)benzylidene-9-arylimino-5,6,7,8-tetrahydrocyclohepta[*b*]pyridyliron(II) precatalysts toward ethylene polymerization and highly linear polyethylenes, J. Polym. Sci, Part A: Polym. Chem. 55 (2017) 830–842.
64. Z. Wang, G. A. Solan, Q. Mahmood, Q. Liu, Y. Ma, X. Hao, W.-H. Sun, Bis(imino)pyridines incorporating doubly fused eight-membered rings as conformationally flexible supports for cobalt ethylene polymerization catalysts, Organometallics 37 (2018) 380-389.
65. H. Suo, I. I. Oleynik, C. Bariashir, I. V. Oleynik, Z. Wang, G. A. Solan, Y. Ma, T. Liang, W.-H. Sun, Strictly linear polyethylene using Co-catalysts chelated by fused bis(arylimino)pyridines: Probing *ortho*-cycloalkyl ring-size effects on molecular weight, Polymer 149 (2018) 45–54.
66. C. Bariashir, Z. Wang, H. Suo, M. Zada, G. A. Solan, Y. Ma, T. Liang, W.-H. Sun, Narrow dispersed linear polyethylene using cobalt catalysts bearing cycloheptyl-fused bis(imino)pyridines; probing the effects of *ortho*-benzhydryl substitution, Eur. Polym. J. 110 (2019) 240–251.

67. C. Bariashir, Z. Wang, S. Du, G. A. Solan, C. Huang, T. Liang, W.-H. Sun, Cycloheptyl-fused NNO-ligands as electronically modifiable supports for M(II) (M = Co, Fe) chloride precatalysts; probing performance in ethylene oligo-/polymerization, J. Polym. Sci. A Polym. Chem. 55 (2017) 3980–3989.
68. W. Zhang, W.-H. Sun, X. Tang, T. Gao, S. Zhang, P. Hao, J. Chen, Chromium complexes ligated by 2-carbethoxy-6-iminopyridines: Synthesis, characterization and their catalytic behavior toward ethylene polymerization, J. Mol. Catal. A: Chem. 265 (2007) 159–166.
69. G. J. P. Britovsek, S. Mastroianni, G. A. Solan, S. P. D. Baugh, C. Redshaw, V. C. Gibson, A. J. P. White, D. J. Williams, M. R. J. Elsegood, Oligomerisation of ethylene by bis(imino)pyridyliron and -cobalt complexes, Chem. Eur. J. 6 (2000) 2221–2231.
70. X. Cao, F. He, W. Zhao, Z. Cai, X. Hao, T. Shiono, C. Redshaw, W.-H. Sun, 2-[1-(2,6-dibenzhydryl-4-chlorophenylimino)ethyl]-6-[1-(arylimino)ethyl]pyridyliron(II) dichlorides: Synthesis, characterization and ethylene polymerization behavior, Polymer 53 (2012) 1870–1880.

Captions of Chart, Scheme, Figures and Tables

Chart 1 Bis(imino)pyridine-chromium(III) chloride **A** and its fused derivatives, **B** - **F**

Scheme 1 One-pot template route to **Cr1** - **Cr6**

Figure 1 ORTEP representation of **Cr1**. Thermal ellipsoids are shown at the 30% probability and the hydrogen atoms have been omitted for clarity.

Figure 2 Catalytic activity and molecular weight (M_w) versus (a) run temperature (b) Al:Cr molar ratio and (c) run time with **Cr1**/MMAO as the catalyst.

Figure 3 Comparison of the catalytic activities and molecular weights of the polyethylene generated using **Cr1** - **Cr6** with $\mathbf{E}_{2,4,6\text{-Me3Ph}}$; MMAO used as the co-catalyst with other conditions the same.

Figure 4 Catalytic activity and molecular weight (M_w) versus (a) run temperature (b) Al:Cr molar ratio and (c) run time with **Cr1**/MAO as the catalyst.

Figure 5 ^{13}C NMR spectrum of the polyethylene obtained using **Cr1**/MMAO at 20 °C (entry 8, Table 4) and an insert of the upfield region of the spectrum of the polymer obtained using **Cr1**/MAO at 30 °C (entry 9, Table 5); both recorded in 1,1,2,2-tetrachloroethane-d_2 at 135 °C (δ_c73.8).

Table 1 Crystal data and structure refinement for **Cr1**

Table 2 Selected lengths (Å) and angles (°) for **Cr1**

Table 3 Ethylene polymerization screen using **Cr1** with various co-catalysts[a]

Table 4 Ethylene polymerization using **Cr1** – **Cr6**/MMAO[a]

Table 5 Ethylene polymerization using **Cr1 – Cr6**/MAO[a]

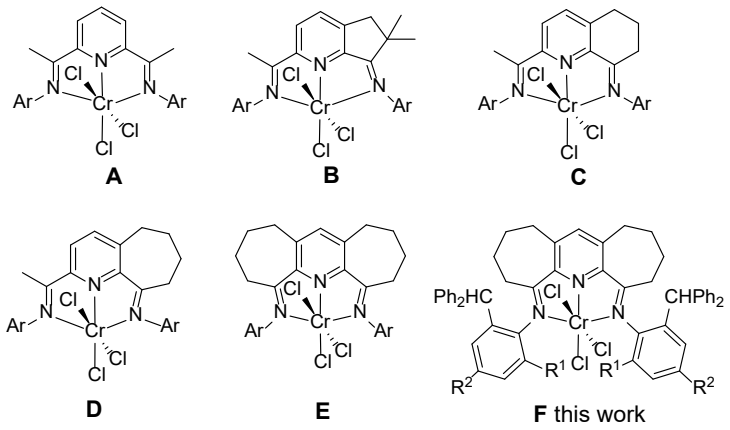

Chart 1 Bis(imino)pyridine-chromium(III) chloride **A** and its fused derivatives, **B - F**

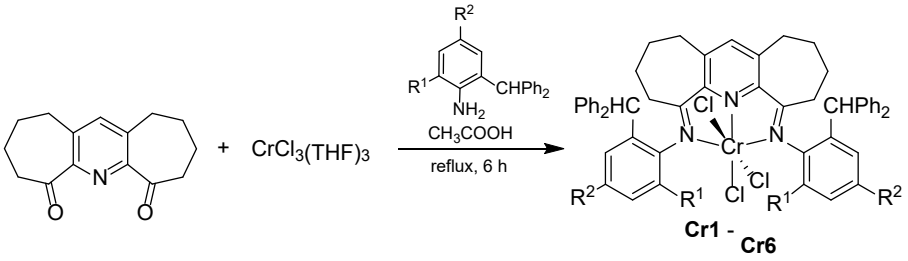

	Cr1	Cr2	Cr3	Cr4	Cr5	Cr6
R^1	Me	Me	Et	*i*-Pr	Cl	F
R^2	Me	Ph_2CH	Ph_2CH	Ph_2CH	Ph_2CH	Ph_2CH
Yield (%)	76	34	30	41	36	80

Scheme 1 One-pot template route to **Cr1 - Cr6**

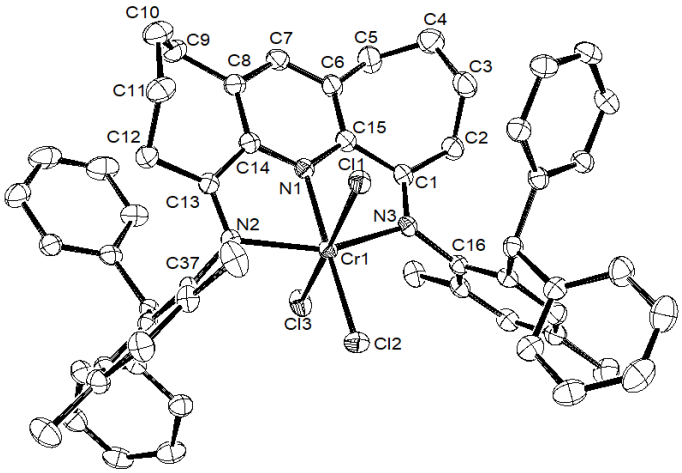

Figure 1 ORTEP representation of **Cr1**. Thermal ellipsoids are shown at the 30% probability and the hydrogen atoms have been omitted for clarity.

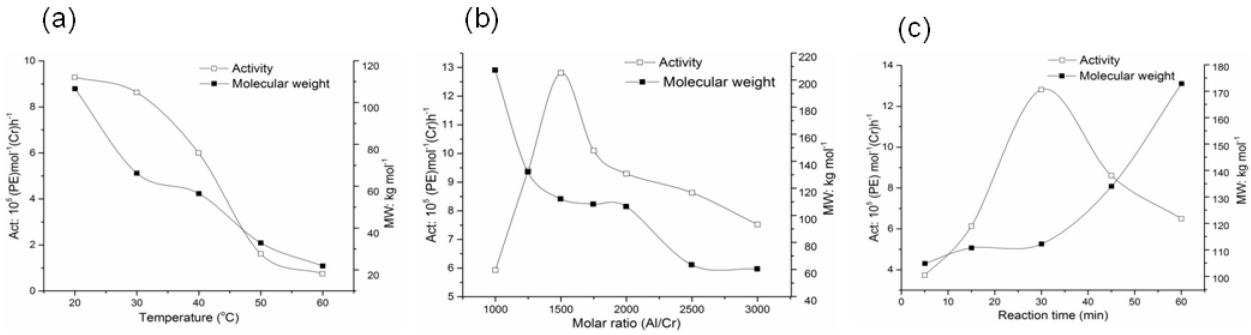

Figure 2 Catalytic activity and molecular weight (M_w) versus (a) run temperature (b) Al:Cr molar ratio and (c) run time with **Cr1**/MMAO as the catalyst.

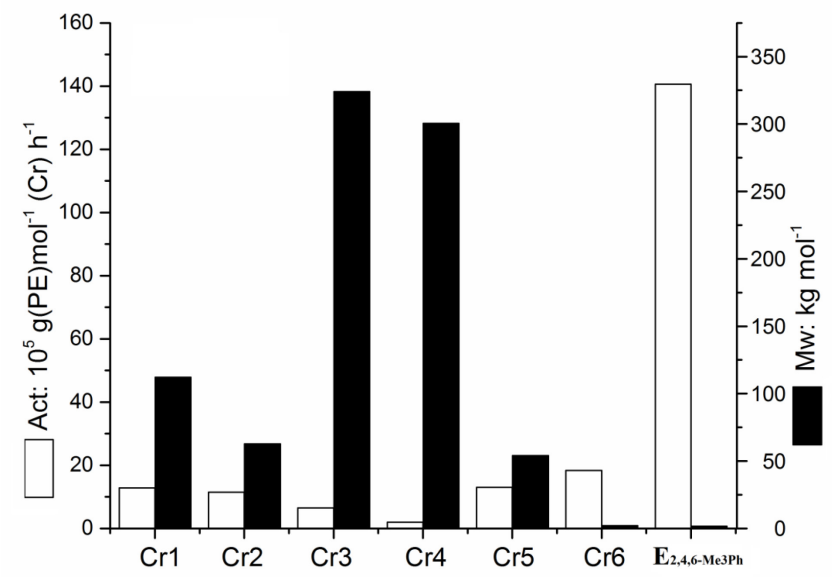

Figure 3 Comparison of the catalytic activities and molecular weights of the polyethylene generated using **Cr1** - **Cr6** with $\mathbf{E}_{2,4,6\text{-Me3Ph}}$; MMAO used as the co-catalyst with other conditions the same.

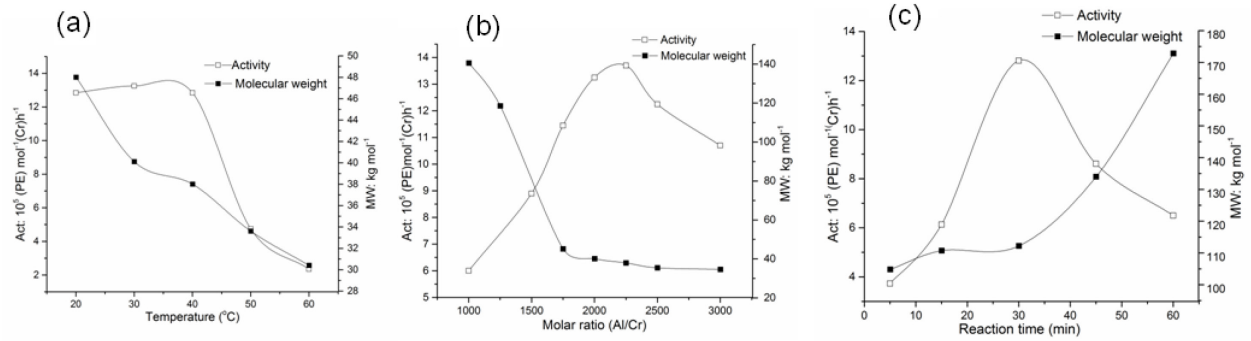

Figure 4 Catalytic activity and molecular weight (M_w) versus (a) run temperature (b) Al:Cr molar ratio and (c) run time with **Cr1**/MAO as the catalyst.

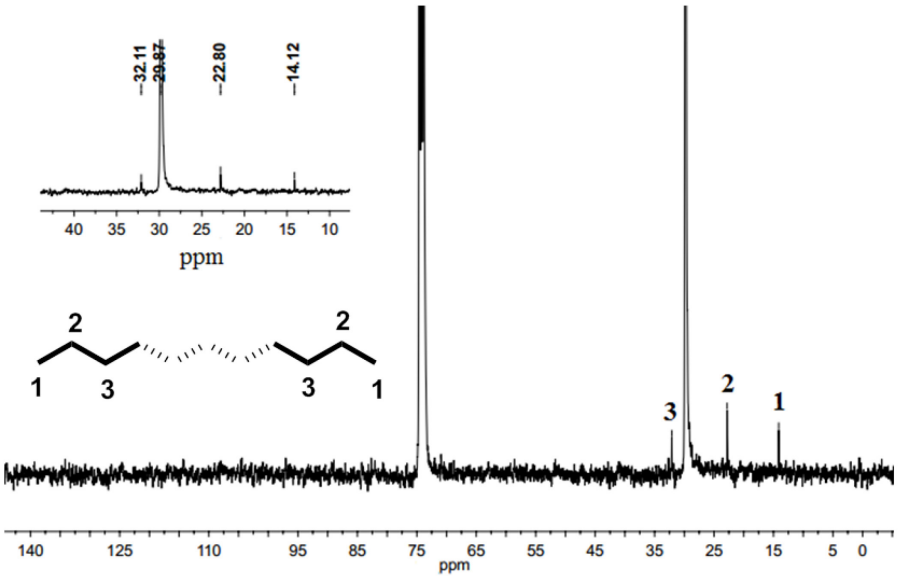

Figure 5 ^{13}C NMR spectrum of the polyethylene obtained using **Cr1**/MMAO at 20 ºC (entry 8, Table 4) and an insert of the upfield region of the spectrum of the polymer obtained using **Cr1**/MAO at 30 ºC (entry 9, Table 5); both recorded in 1,1,2,2-tetrachloroethane-d_2 at 135 ºC (δ_c73.8).

Table 1 Crystal data and structure refinement for **Cr1**

Empirical formula	$C_{57}H_{55}Cl_3CrN_3$
F_w	940.39
T (K)	173.15
Wavelength	0.71073
Crystal system	Monoclinic
Space group	$P2_1/c$
a(Å)	16.7849(7)
b(Å)	18.9573(5)
c(Å)	17.3335(8)
α(°)	90.00
β(°)	117.320(5)
γ(°)	90.00
V(Å^3)	4900.2(4)
Z	4
D_{calcd} (mg m^3)	1.275
μ(mm^{-1})	0.438
F(000)	1972.0
Crystal size (mm)	0.218 × 0.211 × 0.184
θ range (°)	3.408 to 54.97
Limiting indices	$-21 \le h \le 21$
	$-24 \le k \le 24$
	$-22 \le l \le 22$
No. of rflns collected	68482
No. unique rflns [R(int)]	11234 (0.0816)
Completeness to θ (%)	100
Data/restraints/params	11234 / 0 / 581
Goodness of fit on F^2	1.025
Final R indexes [I>=2σ (I)]	R_1 = 0.0608
	wR_2 = 0.1317
R indexes (all data)	R_1 = 0.0965
	wR_2 = 0.1490
Largest diff peak and hole (e Å^{-3})	0.77 and -0.36

Table 2 Selected lengths (Å) and angles (°) for **Cr1**

Bond lengths [Å]		Bond angles [°]	
Cr(1)-N(1)	2.007(2)	N(3)-Cr(1)-N(1)	77.74(9)
Cr(1)-N(2)	2.127(2)	N(2)-Cr(1)-N(1)	77.44(9)
Cr(1)-N(3)	2.126(2)	N(2)-Cr(1)-N(3)	154.80(9)
Cr(1)-Cl(1)	2.3352(8)	N(1)-Cr(1)-Cl(1)	81.63(7)
Cr(1)-Cl(2)	2.2923(8)	N(2)-Cr(1)-Cl(1)	89.89(6)
Cr(1)-Cl(3)	2.2954(8)	N(3)-Cr(1)-Cl(1)	90.82(6)
N(2)-C(13)	1.299(3)	N(1)-Cr(1)-Cl(2)	174.38(7)
N(3)-C(1)	1.295(4)	N(1)-Cr(1)-Cl(3)	93.49(7)
N(1)-C(15)	1.344(3)	N(2)-Cr(1)-Cl(3)	91.18(6)
N(1)-C(14)	1.346(3)	N(2)-Cr(1)-Cl(2)	101.29(7)
N(3)-C(16)	1.464(3)	N(3)-Cr(1)-Cl(2)	103.83(7)
N(2)-C(37)	1.460(3)	N(3)-Cr(1)-Cl(3)	85.98(6)

Table 3 Ethylene polymerization screen using **Cr1** with various co-catalysts[a]

Entry	Co-cat.	Al:Cr	Mass of PE (g)	Activity[b]	M_w[c]	M_w/M_n[c]	T_m[d] (°C)
1	MAO	2000	1.73	8.63	40.1	2.5	132.2
2	MMAO	2000	2.65	13.25	66.2	9.3	132.9
3	Et_2AlCl	400	0.31	1.56	650.3	7.3	135.1
4	EASC	400	0.20	1.00	652.3	7.8	135.0

[a] Conditions: 4.0 μmol of **Cr1**, 100 mL toluene, 10 atm ethylene, 30 °C, 30 min.

[b] Values in units of 10^5 g(PE) mol^{-1}(Cr) h^{-1}.

[c] Determined by GPC, and M_w: kg mol^{-1}.

[d] Determined by DSC.

Table 4 Ethylene polymerization using **Cr1 – Cr6**/MMAO[a]

Entry	Precat.	Al:Cr	T (°C)	t (min)	Mass of PE (g)	Activity[b]	M_w[c]	M_w/M_n[c]	T_m[d] (°C)
1	**Cr1**	2000	20	30	1.86	9.29	106.6	4.9	134.1
2	**Cr1**	2000	30	30	1.73	8.63	66.2	9.3	132.2
3	**Cr1**	2000	40	30	1.20	6.00	56.5	3.2	133.1
4	**Cr1**	2000	50	30	0.32	1.62	32.9	2.8	132.7
5	**Cr1**	2000	60	30	0.15	0.75	21.9	10.3	130.6
6	**Cr1**	1000	20	30	1.19	5.93	207.3	6.2	133.9
7	**Cr1**	1250	20	30	1.88	9.40	132.2	2.8	134.1
8	**Cr1**	1500	20	30	2.56	12.81	112.2	3.0	133.5
9	**Cr1**	1750	20	30	2.02	10.1	108.3	2.7	133.6
10	**Cr1**	2500	20	30	1.61	8.63	63.5	2.3	133.0
11	**Cr1**	3000	20	30	1.50	7.52	60.4	2.6	133.1
12	**Cr1**	1500	20	5	0.12	3.73	104.8	3.9	133.7
13	**Cr1**	1500	20	15	0.61	6.13	110.7	2.9	133.4
14	**Cr1**	1500	20	45	2.58	8.61	134.0	4.2	133.8
15	**Cr1**	1500	20	60	2.60	6.50	172.8	7.2	133.0
16[e]	**Cr1**	1500	20	30	0.76	3.80	67.7	2.5	132.7
17[f]	**Cr1**	1500	20	30	Trace	Trace	-	-	-
18	**Cr2**	1500	20	30	2.30	11.50	62.8	2.4	133.1
19	**Cr3**	1500	20	30	1.29	6.45	294.1	7.5	133.4
20	**Cr4**	1500	20	30	0.39	1.95	300.4	9.7	134.1
21	**Cr5**	1500	20	30	2.60	13.02	54.0	3.0	134.2
22	**Cr6**	1500	20	30	3.66	18.33	2.17	1.8	123.0

[a] Conditions: 4.0 μmol of chromium precatalyst, 100 mL toluene, 10 atm C_2H_4.
[b] Values in units of 10^5 g(PE) mol^{-1} (Cr) h^{-1} .
[c] Determined by GPC, and M_w: kg mol^{-1}.
[d] Determined by DSC.
[e] 5 atm C_2H_4.
[f] 1 atm C_2H_4.

Table 5 Ethylene polymerization using **Cr1** – **Cr6**/MAO[a]

Entry	Precat.	Al:Cr	T (°C)	t (min)	Mass of PE (g)	Activity[b]	M_w[c]	M_w/M_n[c]	T_m[d] (°C)
1	**Cr1**	2000	20	30	2.57	12.85	48.0	2.56	132.8
2	**Cr1**	2000	30	30	2.65	13.25	40.1	2.53	132.9
3	**Cr1**	2000	40	30	2.57	12.85	38.0	2.61	132.2
4	**Cr1**	2000	50	30	0.95	4.75	33.6	7.56	134.2
5	**Cr1**	2000	60	30	0.47	2.35	n.d	-	131.5
6	**Cr1**	1000	30	30	1.20	6.00	140.5	4.68	135.9
7	**Cr1**	1500	30	30	1.78	8.90	118.5	2.74	134.0
8	**Cr1**	1750	30	30	2.29	11.45	45.1	2.29	133.9
9	**Cr1**	2250	30	30	2.74	13.70	37.9	2.02	132.7
10	**Cr1**	2500	30	30	2.45	12.25	35.4	2.12	132.6
11	**Cr1**	3000	30	30	2.14	10.70	34.6	2.49	132.0
12	**Cr1**	2250	30	5	0.18	5.55	32.9	3.50	133.1
13	**Cr1**	2250	30	15	0.85	8.50	36.3	3.08	132.5
14	**Cr1**	2250	30	45	2.86	9.52	65.4	5.84	132.3
15	**Cr1**	2250	30	60	3.48	8.70	69.4	6.05	132.4
16[e]	**Cr1**	2250	30	30	0.92	4.60	34.8	4.56	132.0
17[f]	**Cr1**	2250	30	30	Trace	Trace	-	-	-
18	**Cr2**	2250	30	30	2.56	12.80	68.7	3.98	130.4
19	**Cr3**	2250	30	30	1.99	9.93	75.9	2.79	132.3
20	**Cr4**	2250	30	30	0.66	3.30	270.4	4.74	133.5
21	**Cr5**	2250	30	30	2.78	13.90	36.2	3.08	134.1
22	**Cr6**	2250	30	30	3.43	17.15	2.29	2.05	123.4

[a] Conditions: 4.0 μmol of chromium precatalyst, 100 mL toluene, 10 atm C_2H_4.
[b] Values in units of 10^5 g(PE) mol^{-1} (Cr) h^{-1} .
[c] Determined by GPC, and M_w: kg mol^{-1}.
[d] Determined by DSC.
[f] 1 atm C_2H_4.